energies

MDPI

Article

Influence of the Semiconductor Devices Cooling Conditions on Characteristics of Selected DC–DC Converters

Krzysztof Górecki

Katedra Elektroniki Morskiej, Uniwersytet Morski w Gdyni, Morska 83, 81-225 Gdynia, Poland; k.gorecki@we.umg.edu.pl

Abstract: The problem of an influence of cooling conditions of power semiconductor devices on properties of selected DC–DC converters is considered. The new version of electrothermal average model of a diode-transistor switch for SPICE (Simulation Program with Integrated Circuit Emphasis) is used in the investigations. This model makes it possible to take into account thermal inertia of semiconductor devices as well as mutual thermal interactions between these devices. The investigations are performed for boost and buck converters containing the power MOS (Metal-Oxide-Semiconductor) transistor and the diode. Computational results obtained using the proposed model are shown and discussed. Particularly, an influence of thermal phenomena in the diode and the power MOS transistor on the converters output voltage and internal temperature of the semiconductor devices is considered. The correctness of the selected results of computations was verified experimentally.

Keywords: DC–DC converters; modelling; SPICE; electrothermal models; power semiconductor de vices; averaged models; diode-transistor switch

Citation: Górecki, K. Influence of the Semiconductor Devices Cooling Conditions on Characteristics of Selected DC–DC Converters. *Energies* **2021**, *14*, 1672. https://doi.org/10.3390/en14061672

Academic Editor: Byoung Kuk Lee

Received: 8 February 2021
Accepted: 12 March 2021
Published: 17 March 2021

1. Introduction

DC–DC converters are the basic component of switch-mode power supplies [1–6]. Such converters contain at least one diode and one transistor. Internal temperature of the mentioned semiconductor devices increases while they operate. This is a result of thermal phenomena—self-heating in both the devices as well as and mutual thermal couplings between the diode and the transistor operating on a common base. It can be a heat-sink or a printed circuit board (PCB) [7–13].

In order to effectively design and analyze properties of electronic networks, computer simulations are used [2,14–17]. Such simulations require models of all components of the analyzed network. The accuracy of the obtained computation results is determined by the accuracy of the used models of the components of the analyzed network.

While performing computer simulations, one should pay attention to two basic parameters: the accuracy of the obtained computation results and the duration time of these computations [14,15,17,18]. Therefore, different models and analysis methods are used at various stages of a designing process of electronic components, circuits and systems. It is also important to select the software that performs these computations. In the analysis of power electronics systems, the SPICE software is commonly used [14,19].

For DC–DC converters, which belong to the group of switch-mode systems, the natural method of determining their characteristics is a transient analysis. However, such an analysis, performed using physical models of semiconductor devices, is very time consuming. The long duration time of such an analysis is caused by large differences, up to 9 orders of magnitude, between electric time constants of the semiconductor devices, electric time constants related to the LC components contained in the converter and the thermal time constants of the used cooling system [7,20]. Using the classical method of a transients analysis in the SPICE software and the semiconductor devices electrothermal models given in the literature [9,21–25], the duration time of computations would be unacceptably long [26]. Therefore, in the literature [7,16,27] some special algorithms that

enable quick computation of time waveforms of voltages and currents in the considered class of systems in the steady state can be found. These methods, however, require the use of special algorithms predicting the solution that use programs that are not commonly available.

When designing the class of the considered networks, the idea of averaged models is often used, which allow determining the average values of voltages and currents in the analyzed networks at the steady state [1,14,28–34]. Typically, in such models, the semiconductor devices are represented by ideal switches or two-value resistors [1,14]. The previous articles by the author [10,30,35,36] proposed the averaged electrothermal models of boost or buck converters for SPICE which take into account the phenomenon of self-heating in the diode, the MOS (Metal-Oxide-Semiconductor) transistor or the IGBT on the characteristics of these converters. These models make also possible to compute the internal temperature of these semiconductor devices. The usefulness of the proposed models was experimentally demonstrated in the cited articles, but the experimental verification was performed only for the thermally steady state using the DC analysis in SPICE.

As it was indicated, e.g., in the book [14], the frequency characteristics of the considered class of switch-mode power converters and the waveforms of the average voltage and current values can be also computed using the averaged models. Using the idea of electrothermal averaged model of a diode-transistor switch (DTS) proposed earlier in the article [30], it is possible to formulate an electrothermal averaged model of any DC–DC converter taking into account the influence of the properties of the semiconductor devices cooling system on the characteristics of these converters.

This article proposes a new averaged electrothermal model of a diode-transistor switch for SPICE. This model takes into account thermal inertia of the diode and the transistor and mutual thermal couplings between these devices. The proposed model makes it possible to compute waveforms of electrical parameters of the investigated DC–DC converters and internal temperature of semiconductor devices. Using this model, the influence of the cooling conditions of the diode and the MOS power transistor on the characteristics of buck and boost converters is analyzed. The selected results of the calculations are verified experimentally.

Section 2 presents the form of the formulated model. Section 3 contains a description of the tested converters and their simulation model. The investigation results showing the influence of the applied cooling system on the properties of the modelled networks are presented and discussed in Section 4.

2. Model Form

The proposed model of DTS is formulated on the basis of the observation given, e.g., in [1,14,28,29,33] that in each DC–DC converter with the single-inductor the component consisting of a diode and a transistor is used. The new version of the electrothermal model of the diode-transistor switch is formulated as a subcircuit for the SPICE software. It is an extended version of the model described in [30]. In comparison to the cited paper, the new model allows taking into account the influence of thermal inertia of the diode and the transistor as well as thermal couplings between them on the mean values and the waveforms of voltages and currents in the analyzed networks and the internal temperatures of mentioned semiconductor devices.

The network form of the proposed model is presented in Figure 1.

The proposed model contains four following blocks: Main circuit, CCM/DCM, Aided block and Thermal model. Main circuit describes the voltage between drain (D) and source (S) of the power MOS transistor and the current flowing through the diode connected between anode (A) and cathode (C). Instead of the transistor gate terminal, there is a d terminal, to which the voltage corresponding to the duty cycle of the signal which controls the gate of the applied transistor is connected.

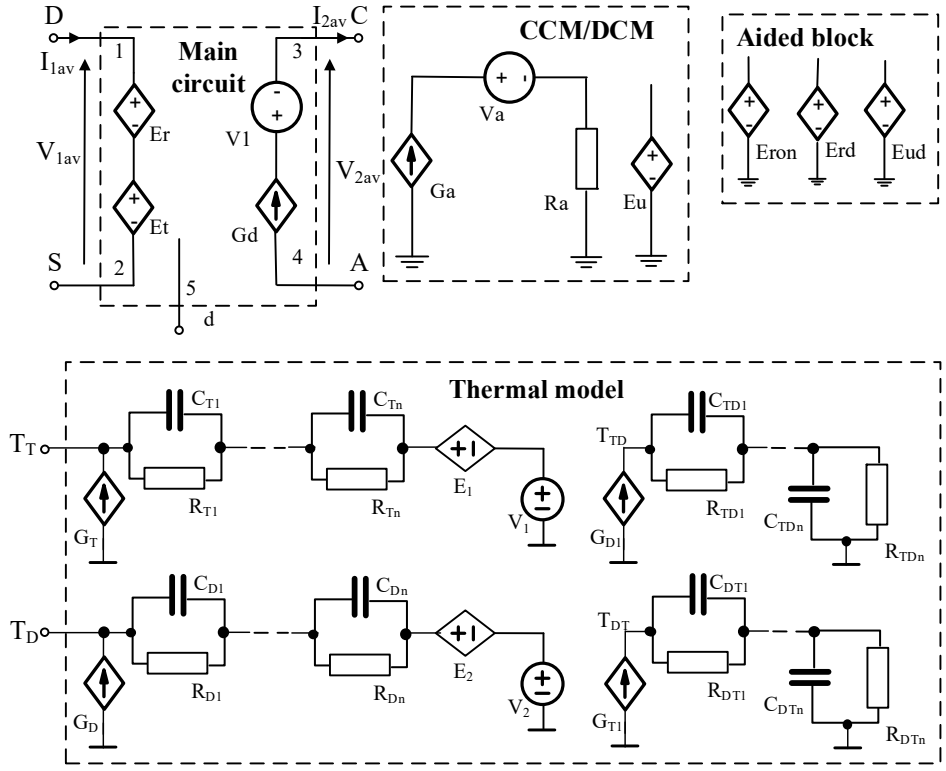

Figure 1. Network representation of the electrothermal average model of diode-transistor switch (DTS).

In Main circuit the controlled voltage sources Er and Et connected in series model the average value of the drain-source voltage of the unipolar transistor between terminals D and S. Two components: the controlled current source Gd and voltage source V1 connected between terminals A and C models the diode. CCM/DCM block contains 4 components: the resistor Ra, the voltage source Va, the controlled current source Ga and the controlled voltage source Eu. These components are needed to determine the operation mode of the DC–DC converter with the considered switch. The controlled voltage source Eu generates voltage, the value of which depends on the duty cycle d and frequency f of the control signal, on the output current and inductance of the inductor contained in the modelled DC–DC converter.

Aided block contains three controlled voltage sources Eud, Eron and Erd. These components model the dependences of: the forward voltage of the diode, on-state resistance of the transistor and diode series resistance on temperature. Voltages on the mentioned voltage sources are used to control the voltage and current sources included in Main circuit and described in detail in [30]. In this description internal temperatures of the transistor T_T or of the diode T_D occur. The values of these internal temperatures are computed in Thermal model.

In Thermal model, the temperatures inside the transistor and the diode are determined and the focused thermal model is used [37–41]. This model takes into account self-heating in each of the semiconductor devices mentioned and mutual thermal couplings between them. It uses an idea of self and transfer transient thermal impedances, described e.g., in the papers [41,42].

The transistor internal temperature T_T at time t is calculated using following equation

$$T_T(t) = T_a + \int_0^t Z'_{thT}(t-v)\cdot p_T(v)\,dv + \int_0^t Z'_{thTD}(t-v)\cdot p_D(v)\,dv \quad (1)$$

where T_a denotes ambient temperature, p_T and p_D—power dissipated in the transistor and in the diode, respectively, $Z'_{thT}(t)$—time derivative of the transistor transient thermal impedance, and $Z'_{thTD}(t)$—time derivative of the transfer transient thermal impedance between the transistor and the diode. The diode internal temperature T_D is expressed by the relationship analogous to that given by the Equation (1), where the index T should be replaced with the index D.

The transient thermal impedances used in the presented model and the transfer transient thermal impedance are described by the dependence [37,38]

$$Z_{th}(t) = R_{th} \cdot \left(1 - \sum_{i=1}^{N} a_i \cdot \exp\left(-\frac{t}{\tau_{thi}}\right)\right) \tag{2}$$

where R_{th} is thermal resistance, a_i is the weighting factor associated with the thermal time constant τ_{thi}, and N is the number of thermal time constants.

In Thermal model presented in Figure 1, the circuits on the left side model the self-heating phenomenon, and the circuits on the right-side—the mutual thermal coupling. The current sources G_T and G_{T1} describe the average value of the power dissipated in the power MOS transistor, the current sources G_D and G_{D1}—the average value of the power dissipated in the diode. The voltage on the voltage sources V_1 and V_2 corresponds to ambient temperature T_a. The controlled voltage sources E_1 and E_2 model a temperature increase of transistor T_{TD} and diode T_{DT} caused by mutual thermal couplings. The RC elements model particular transient thermal impedances. Thermal resistance R_i and thermal capacitance C_i are given by the equations of the form

$$R_i = a_i \cdot R_{th} \tag{3}$$

$$C_i = \frac{\tau_{thi}}{a_i \cdot R_{th}} \tag{4}$$

The parameters R_{th}, a_i and τ_{thi} appearing in the Equations (3) and (4) correspond to the individual thermal transient impedances occurring in the presented model. These parameters values are determined using the measurements results of these transient thermal impedances made using indirect electrical methods described, among others in the papers [41,43]. Using these results and the ESTYM algorithm described in [37], values of the parameters included in the Equations (3) and (4) are calculated separately for transient thermal impedance of transistor $Z_{thT}(t)$ and diode $Z_{thD}(t)$ and for the transfer transient thermal impedance between these devices $Z_{thTD}(t)$.

3. Investigated Networks

The investigations of an influence of the cooling conditions of semiconductor devices on the characteristics of single-inductor DC–DC converters were performed for classic boost and buck converters containing a power MOS transistor and a diode. The dependence of the inductor inductance on the current was ignored in the investigations. The tested DC–DC converters used an IRF 840 transistor and a BY229 diode.

In order to use the proposed model in the analyses of a DC–DC converter the simulation diagram should be formulated. In this network all the components of the investigated converter should be included, except semiconductor devices. Additionally, the network representation of the diode-transistor switch (DTS) has to be included in this network. The proper terminals of DTS should be connected to the nodes of the investigated DC–DC converter instead of terminals of the diode and the transistor.

The simulation diagrams of the considered converters are shown in Figure 2 (buck converter) and Figure 3 (boost converter). For simplicity, only Main circuit from the model shown in Figure 1 is presented in these figures.

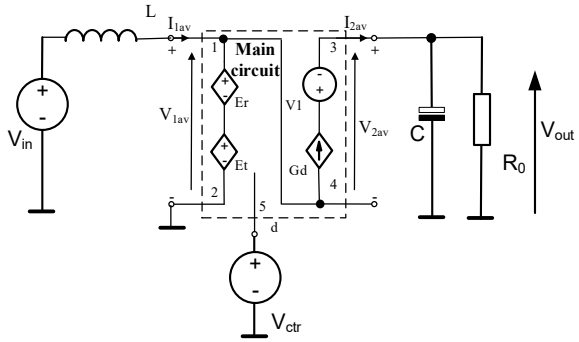

Figure 2. Simulation diagram of the boost converter.

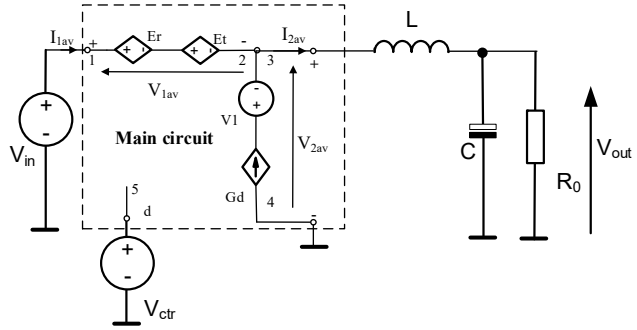

Figure 3. Simulation diagram of the buck converter.

In the considered converters the voltage source V_{in} represents their input voltage, resistor R_0—the converter load, L—the energy storage inductor, C—the capacitor filtering ripples of the output voltage, V_{ctr} models the duty cycle of the control signal. The controlled voltage sources model the MOS transistor, whereas the sources Gd and V1 model the diode.

In the proposed model of DTS, the following values of the parameters characterizing the properties of the power MOS transistor are used: resistance of the switched-on channel at the reference temperature T_0 = 300 K is R_{ON0} = 0.67 Ω, the temperature coefficient of this resistance α_{ON} = 0.01 K^{-1}. In turn, the diode forward voltage at temperature T_0 is V_{D0} = 0.88 V, the diode series resistance at temperature T_0 is equal to R_{DO} = 0.12 Ω, the temperature coefficient of forward voltage $\alpha_U = -2$ mV/K, whereas the temperature coefficient of series resistance α_{RD} = 0.003 K^{-1}.

4. Investigations Results

The papers [30,32] present the results of investigations of the averaged electrothermal model of DTS. In the cited papers only the operation of buck or boost converters at the thermally steady state under one set of cooling conditions of the transistor and the diode was considered. This section contains the results of computations and measurements of the above-mentioned DC–DC converters operating under different cooling conditions of the IRF840 transistor and the BY229 diode. In all the figures shown in this section, points denote the measurements results, and lines—the computations results carried out using the proposed model. The computations were performed using the PC with the Procesor Intel(R) Core(TM) i3-8130U CPU@2.20 GHz, 2208 MHz, 2 cores.

Figure 4 shows the measured and computed dependences of the output voltage of the boost converter on the duty cycle d of the control signal (Figure 4a) and on load resistance (Figure 4b). The investigations were performed for the fixed values of voltage V_{in} and period T_S of the control signal. Thermal resistance had the following values: R_{thT} = 8 K/W and R_{thD} = 12 K/W for the devices situated on the heat-sink and R_{thT} = 55 K/W and R_{thD} = 20 K/W for the devices operating without any heat-sink. Inductor L had inductance equal to 650 μH and series resistance equal to 0.1 Ω. In turn, capacitor C had capacitance equal to 470 μF. The values of voltage V_{in} and period T_S are given in each figure.

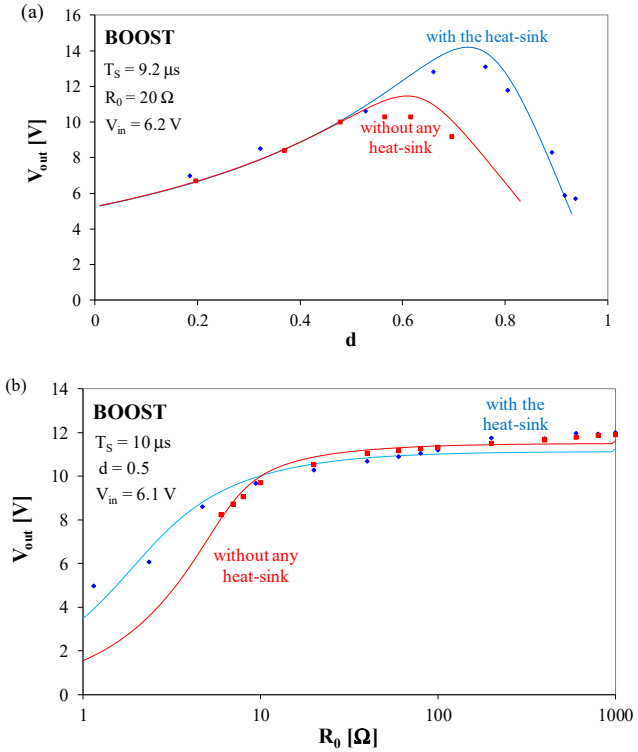

Figure 4. Dependences of the boost converter output voltage on: (**a**) the duty cycle d, (**b**) on load resistance.

As it is seen in Figure 4a, the dependence $V_{out}(d)$ had a maximum. It occurred with d values equal to about 0.6 (for the devices without any heat-sink) and 0.75 for the devices situated on the heat-sink. For d < 0.5, there was practically no influence observed of the cooling conditions of the applied semiconductor devices on the considered dependences. The use of a heat sink allowed obtaining higher values of the d factor, at which the considered converter operated in the safe operation area. In turn, in Figure 4b it is visible that the converter output voltage increased with an increase in load resistance R_0. The influence of the cooling conditions of the semiconductor devices was visible in the resistance range R_0 < 20 Ω. In this range, the use of a heat-sink for the semiconductor devices caused an increase in V_{out} voltage.

Figure 5 shows the dependences of the transistor case temperature on the coefficient d (Figure 5a) and on resistance R_0 (Figure 5b).

The results of computations and measurements of temperature T_{CT} differed only slightly from each other. One should notice that the discrepancies between the values of the considered temperature obtained under various cooling conditions of the transistor exceeded even 100 °C, and a big increase in this temperature limited the permissible range of changes in the coefficient d or resistance R_0 related to the limited permissible value of the transistor internal temperature.

Figures 6 and 7 illustrate the measured and computed characteristics of a buck converter operating at V_{in} = 20.4 V and the control signal frequency wass 100 kHz. Figure 6 shows the dependence of the output voltage of this converter on the duty cycle d (Figure 6a) and load resistance R_0 (Figure 6b). Inductor L had inductance equal to 92 µH and series resistance equal to 0.28 Ω. In turn, capacitor C had capacitance equal to 470 µF.

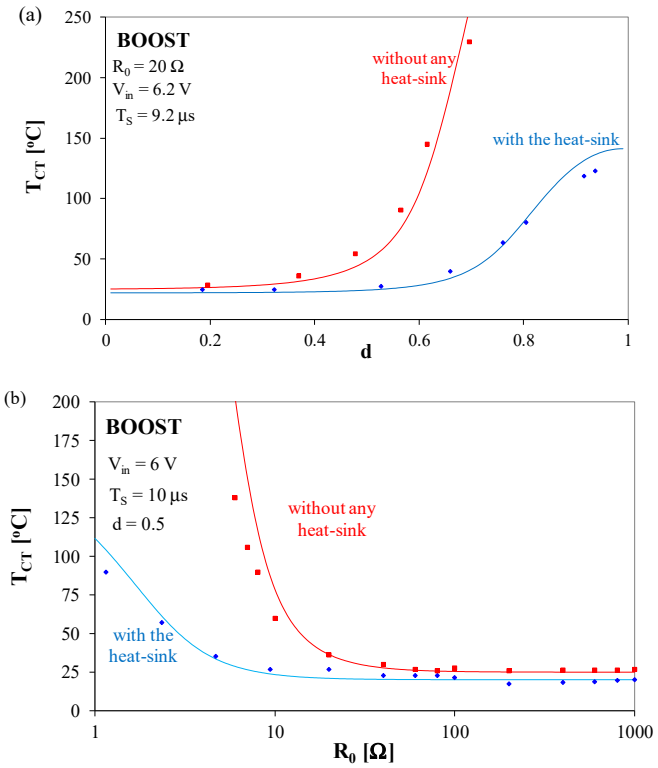

Figure 5. Dependences of the case temperature of the transistor contained in the boost converter on: (**a**) the duty cycle d, (**b**) on load resistance.

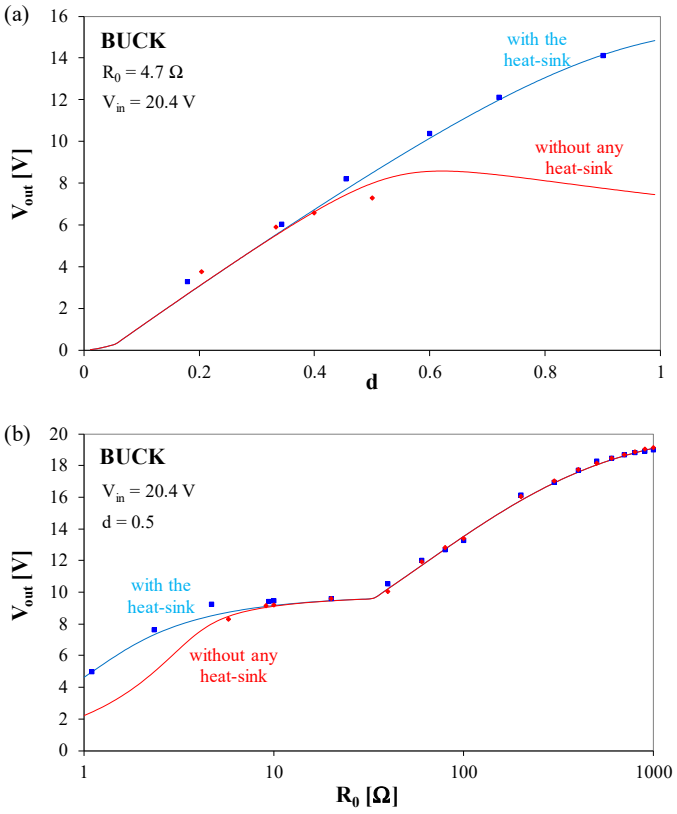

Figure 6. Dependences of the buck converter output voltage on: (**a**) the duty cycle d, (**b**) on load resistance.

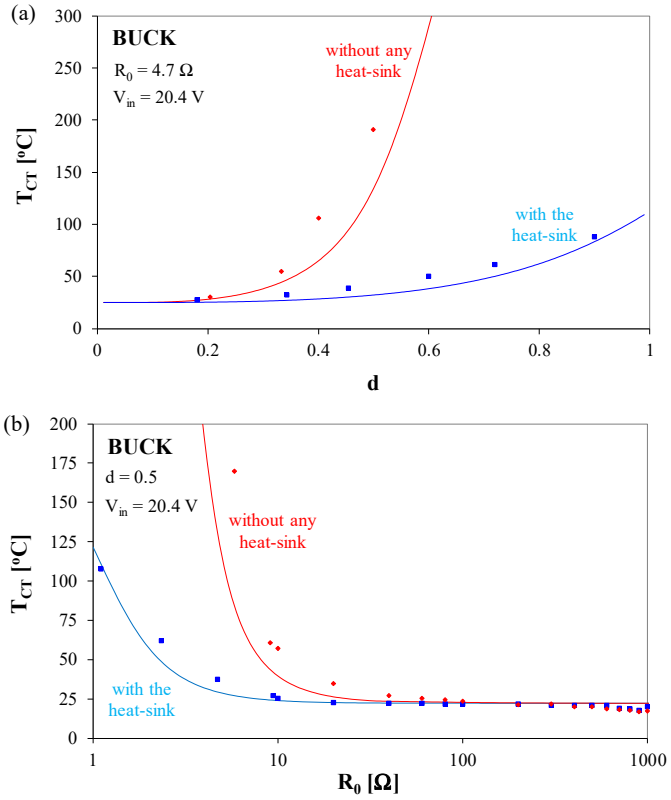

Figure 7. Dependences of the case temperature of the transistor contained in the buck converter on: (**a**) the duty cycle d, (**b**) on load resistance.

As can be observed in Figure 6a, the output voltage was an increasing function of parameter d only for the case where the semiconductor devices were situated on the heat sink. For these devices operating without any heat sink, the maximum of the dependence V_{out}(d) was visible. The discrepancy between the values of voltage V_{out} obtained for both considered set of cooling conditions was an increasing function of the coefficient d. In Figure 6b it is visible that the dependence V_{out} (R_0) was a monotonically increasing function. If $R_0 > 20$ Ω the buck converter operated in Discontinuous Conducting Mode (DCM), and for $R_0 < 20$ Ω—in CCM (Continuous Conducting Mode). The influence of cooling conditions on semiconductor devices was visible only for low values of resistance R_0.

Figure 7 illustrates an influence of the coefficient d (Figure 7a) and resistance R_0 (Figure 7b) on the transistor case temperature.

In Figure 7 it is visible that temperature T_{CT} increased when resistance R_0 decreases or the coefficient d increases. The cooling conditions of the semiconductor devices significantly affected the value of this temperature for high d values and low R_0 values. The cooling conditions of these devices determined the permissible control and load conditions of the buck converter.

The computations and measurements results presented above refer only to the thermally steady state and are obtained using the DC analysis. In all the presented cases, an increase in the internal temperatures of the diode and the transistor was caused exclusively by the self-heating phenomenon in the semiconductor devices that were not embedded in the common substrate. However, the model proposed in Section 2 made it possible to carry out computations that illustrated the impact of thermal inertia and mutual thermal interactions between the diode and the transistor on the characteristics of the investigated converters. Both the used semiconductor devices were mounted in the TO-220 cases. Therefore, in the following considerations it was assumed that for an identical method of

mounting thermal parameters which characterized these semiconductor devices were the same.

Figure 8 shows the measured waveforms of transient thermal impedance of the IRF840 transistor for three sets of the cooling conditions. In this figure the blue line presents results obtained for the transistor situated on the big heat-sink, the black line—for the transistor on the small heat-sink, whereas red line—for the transistor without any heat-sink.

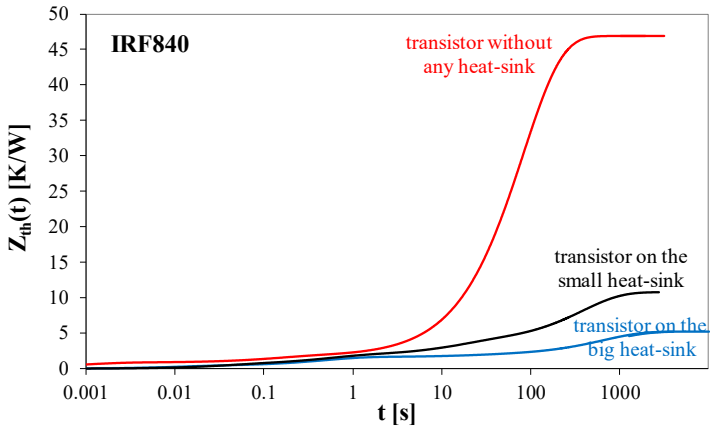

Figure 8. Waveforms of transient thermal impedance of the IRF840 transistor operating at different cooling conditions.

The presented waveforms $Z_{th}(t)$ differed significantly between each other. For example, thermal resistance ranged from 5.16 K/W for the transistor situated on the big heat-sink, through 10.8 K/W for the transistor situated on the small heat-sink, up to 46.9 K/W for the transistor operating without any heat-sink. In turn, the longest thermal time constant, which determined the time of stabilizing the transistor internal temperature, increases from 82 s for the transistor operating without any heat-sink to 765 s for the transistor situated on the big heat-sink.

In turn, the transfer transient thermal impedances between the diode and the transistor situated on the common base were also measured. Figure 9 shows the measurement results normalized to the transistor thermal resistance. The blue line marks the results obtained for the semiconductor devices situated on the common heat-sink, and the red line—the results obtained for the devices mounted on the common PCB.

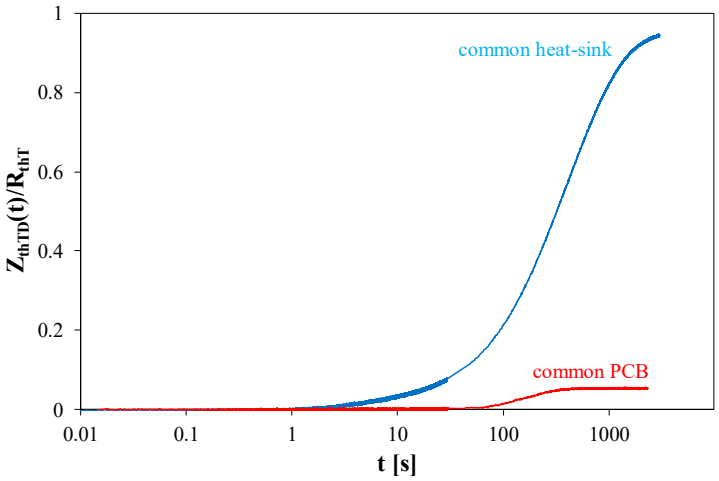

Figure 9. Waveforms of the transfer transient thermal impedance between the transistor and the diode normalized to thermal resistance of the transistor for different cooling conditions.

The influence of the mutual thermal couplings between the considered semiconductor devices was practically negligible when the components were mounted on a common PCB. In this case, the transfer thermal resistance slightly exceeded 5% of thermal resistance of the transistor. The delay in the heat flow between the diode and the transistor was as much as 80 s. On the other hand, for the devices placed on the common heat-sink, the transfer thermal resistance reached even 95% of the transistor thermal resistance. The delay of heat flow was less than 2 s. It can therefore be expected that mutual thermal couplings between the diode and the transistor may have significantly influenced the operation of the DC–DC converters considered in this type of the operation conditions only if these devices were assembled on the common heat-sink.

Using the measured transient thermal impedances of the diode and the transistor and of transfer transient thermal impedance between them, the waveforms of the output voltage of the investigated converters and the internal temperatures of the semiconductor devices contained in these converters were computed. Figures 10 and 11 illustrate the influence of the transistor and diode cooling conditions on characteristics of boost and buck converters. The results of computations presented in these figures were performed neglecting mutual thermal couplings between the diode and the transistor, and the thermal properties of these devices were characterized by waveforms $Z_{th}(t)$ shown in Figure 8.

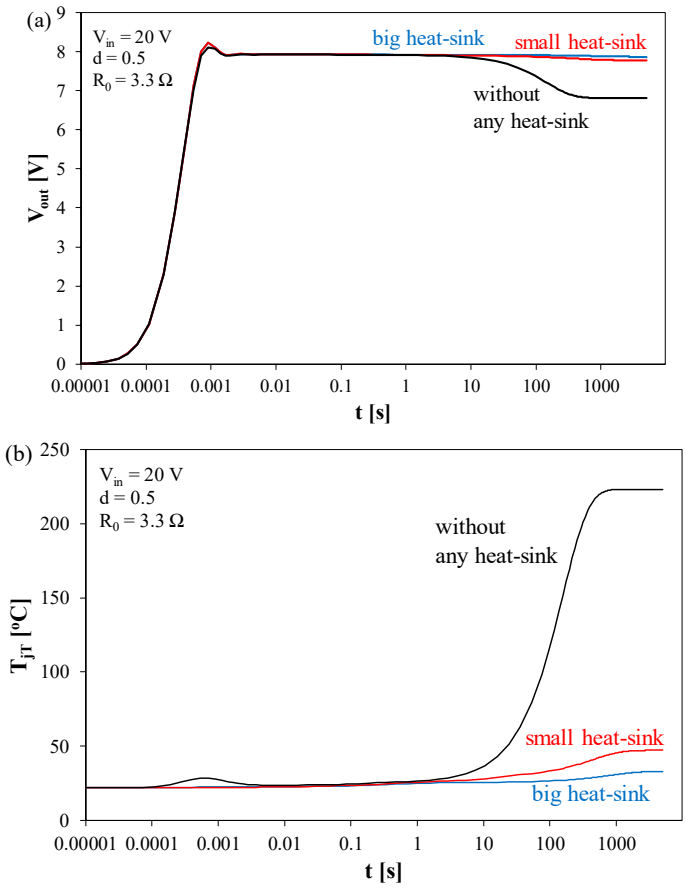

Figure 10. Computed waveforms of: (**a**) the buck converter output voltage at voltage V_{in} of the form of a voltage step, (**b**) the transistor internal temperature.

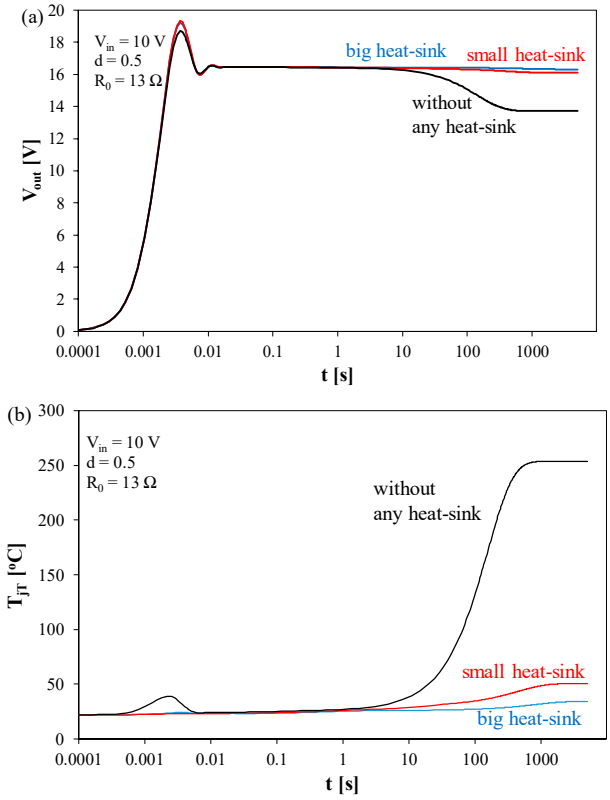

Figure 11. Computed waveforms of: (**a**) the boost converter output voltage at voltage V_{in} of the form of a voltage step, (**b**) the transistor internal temperature.

Figure 10 presents the waveforms of the buck converter output voltage (Figure 10a) and the corresponding to them waveforms of the transistor internal temperature (Figure 10b) obtained when the input voltage V_{in} had the form of a voltage step of the value 20 V. The control signal was characterized by following parameters: d = 0.5, f = 100 kHz. The load resistance is R_0 = 3.3 Ω.

As it can be seen, about 1 ms after the moment of switching-on V_{in} voltage, the electrical steady state occurred in the investigated converter. As a result of self-heating, the internal temperature of the semiconductor devices increased, causing a decrease in the output voltage. This decrease was mainly due to an increase in resistance R_{ON} of the switched-on power MOS transistor caused by an increase in its internal temperature T_T. This increase was the highest if a transistor operates without any heat-sink, and it corresponded to a decrease in the output voltage of about 12%. This voltage took a steady value about 300 s after voltage V_{in} was turned on. On the other hand, for a transistor mounted on one of the considered heat-sinks, an increase in internal temperature and a drop in the converter output voltage were much smaller than for a transistor operating without any heat-sink, but the time of stabilizing the value of voltage V_{out} exceeded even an hour.

Figure 11 presents the computed waveforms of the boost converter output voltage (Figure 11a) and the corresponding to them waveforms of the transistor internal temperature (Figure 11b) obtained after its excitation with the input voltage step V_{in} of 10 V. The control signal was characterized by d = 0.5 and f = 100 kHz, whereas load resistance R_0 = 13 Ω.

It can be noticed that for the tested converter there was an overshoot of the output voltage after a few milliseconds from the moment of switching on voltage V_{in}. It reached even 15% of the value at the steady state. This overshoot was accompanied by a local maximum of the transistor internal temperature, which for this device without any heat-sink reached even 40 °C. Similarly as in the buck converter, self-heating phenomena caused

the boost converter output voltage to drop. This decrease was more visible when the worse cooling conditions were provided for the semiconductor devices. Voltage V_{out} decreased even by 12% for the transistor operating without any heat-sink.

Figures 12 and 13 show characteristics of the investigated converters computed taking into account the influence of mutual thermal couplings between the diode and the transistor.

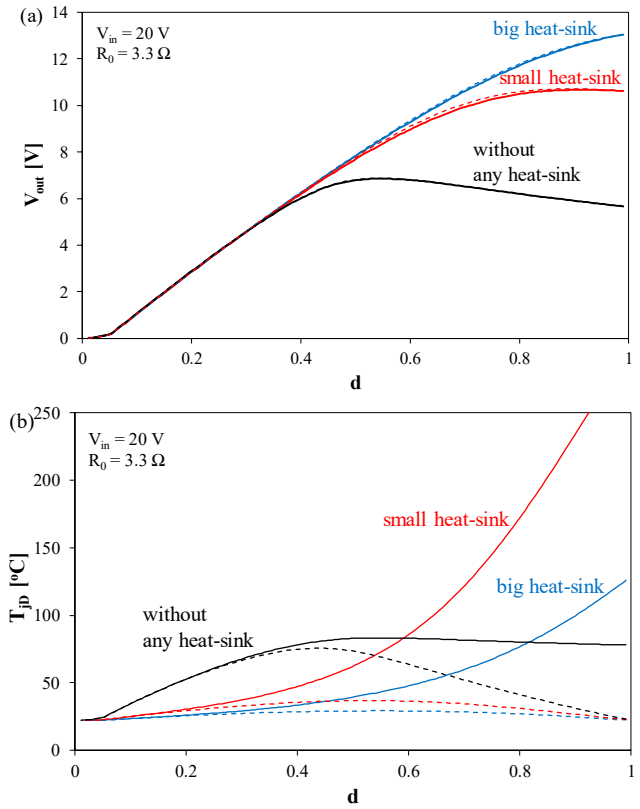

Figure 12. Computed dependences of: (**a**) the buck converter output voltage, (**b**) the diode internal temperature on the duty cycle taking into account mutual thermal interactions between the diode and the transistor.

Figure 12 presents the computed dependences of the buck converter output voltage (Figure 12a) and the diode internal temperature (Figure 12b) on the parameter d. The computations are made taking into account (solid line) and omitting (dashed line) mutual thermal interactions between the diode and the transistor situated on the common: PCB (black lines) or heat-sink (red and blue lines).

As can be seen, practically no influence of the mutual thermal interactions between the diode and the transistor on the dependence of V_{out}(d) was observed. Obviously, for a fixed value of the coefficient d, the output voltage attained higher values for better cooling conditions of the semiconductor devices. For the value of d close to 1, these differences reached even 50%. One should pay attention to the dependence of the diode temperature T_D on the coefficient d. It can be seen that for each of the considered set of the cooling conditions, temperature T_D determined without taking into account thermal interactions between the diode and the transistor was lower than temperature computed while taking into account these interactions. This is due to the diode being heated by a transistor situated on the common base. For the semiconductor devices operating on the common heat-sink and characterized by a higher value of thermal resistance, the considered increase was the highest and even exceeded 200 °C. On the other hand, for semiconductor devices situated on the common PCB, the T_D value increase did not exceed 50 °C. It is also worth noting that the dependence T_D(d) determined without taking into account the thermal interactions

between the semiconductor devices had a maximum with the value of parameter d ranging from 0.4 to 0.6.

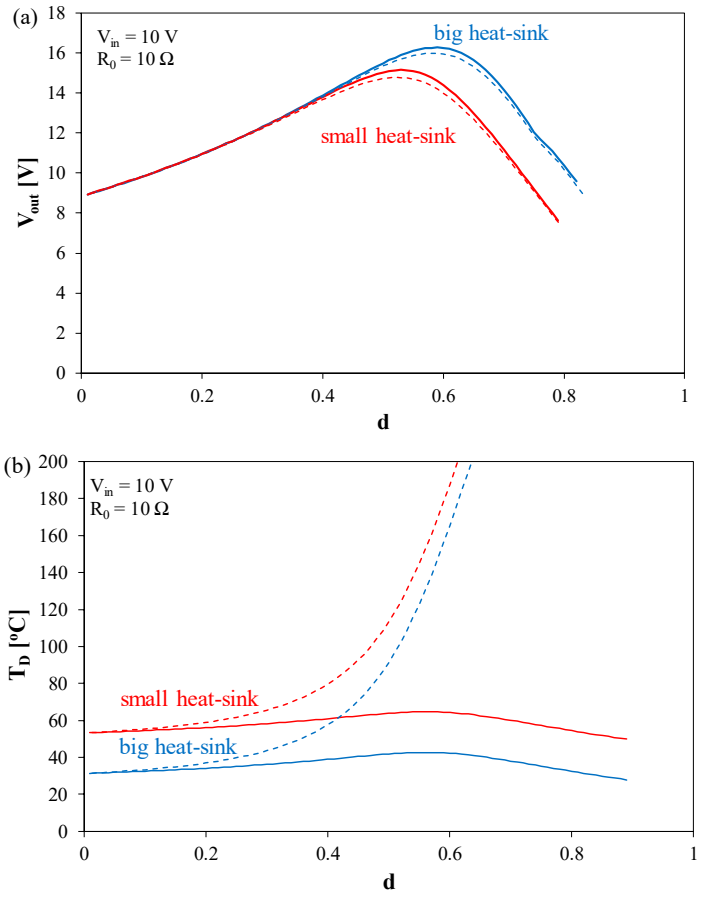

Figure 13. Computed dependences of: (**a**) the boost converter output voltage, (**b**) the diode internal temperature on the duty cycle taking into account mutual thermal interactions between the diode and the transistor.

Figure 13 shows the computed dependences of the boost converter output voltage (Figure 13a) and the diode internal temperature (Figure 13b) on the parameter d. The computations were performed taking into account (dashed line) and omitting (solid line) mutual thermal interactions between the diode and the transistor located on the common heat-sink (red and blue lines).

As can be seen, for all the considered sets of the cooling conditions of the semiconductor devices, the relation $V_{out}(d)$ had a maximum, the value of which increased with the improvement of the cooling conditions. It can also be seen that taking into account mutual thermal interactions between the diode and the transistor caused a significant decrease in the value of the converter output voltage and an increase in the diode internal temperature. Changes in the values of the quantities mentioned were particularly clearly visible for d values above 0.5. In this range, the values of voltage V_{out} computed taking into account thermal interactions between the diode and the transistor and omitting these interactions reached even 0.5 V.

5. Conclusions

The influence of the cooling conditions of the semiconductor devices on properties of selected DC–DC converters is analyzed. A new version of the electrothermal averaged model of DTS was formulated taking into account the effect of mutual thermal couplings between the diode and the transistor and thermal inertia on the properties of the converters containing this switch. Using the developed model, electro-thermal DC analyses and elec-

trothermal transient analyses of the boost and buck converters containing diodes and MOS transistors operating at various cooling conditions were carried out. Selected computation results were compared to the measurement results, obtaining a good agreement between these results.

Due to the use of a new model of a DTS, a very short computation time was obtained, not exceeding 1 s. For comparison, the application of the classical algorithms for the electrothermal transient analysis would require time counted in months.

The obtained results of computations prove that the cooling conditions of the transistor and the diode significantly affect the output voltage of the considered converters. This influence is particularly clear for low load resistance and high values of the parameter d, where the values of this voltage obtained for different sets of the cooling conditions may differ even twice. The cooling conditions of the semiconductor devices significantly affect the permissible range of changes in the coefficient d and resistance R_0, as they determine internal temperature of these devices. As it is known, the permissible value of this temperature is given by the manufacturer and should not be exceeded during operation. The conducted tests confirmed that, under favorable cooling conditions, semiconductor devices can be used in converters operating in a wider range of changes of parameter d and resistance R_0 than at omitting the additional components improving the heat removal.

The range of the allowable d and R_0 values is also limited due to mutual thermal couplings between the diode and the transistor. It is particularly disadvantageous to place these devices on the common heat-sink, because then transfer thermal resistance has a value similar to thermal resistance of the mentioned semiconductor devices. This phenomenon has little influence on the operation of buck and boost converters, in which the diode and the transistor are situated on the common PCB.

It was also shown that due to thermal inertia of the diode and the transistor, the time for stabilizing the output voltage depends on the cooling system used and ranges from a few minutes to an hour. For both the considered converters, a decrease in the the output voltage was observed as a function of time due to the self-heating phenomenon in the diode and in the transistor.

The observed changes in the characteristics of the considered converters result from thermal phenomena occurring in the semiconductor devices, which cause changes in the voltage drop on the forward biased transistors and diodes. The observed changes are particularly important in the case of systems used to feed electronic networks characterized by low voltage and high supply current. The presented investigations results may be useful for designers of this class of electronic systems, enabling the correct selection of semiconductor devices and their cooling systems.

Funding: This research received no external funding.

Institutional Review Board Statement: Not applicable.

Informed Consent Statement: Not applicable.

Data Availability Statement: Data is contained within the article.

Conflicts of Interest: The author declares no conflict of interest.

References

1. Ericson, R.; Maksimovic, D. *Fundamentals of Power Electronics, Norwell*; Kluwer Academic Publisher: Amsterdam, The Netherlands, 2001.
2. Rashid, M.H. *Power Electronic Handbook*; Elsevier: Amsterdam, The Netherlands, 2007.
3. Kazimierczuk, M. *Pulse-Width Modulated DC-DC Power Converters*; Wiley: Hoboken, NJ, USA, 2015.
4. Billings, K.; Morey, T. *Switch-Mode Power Supply Handbook*; McGraw-Hill Companies: New York, NY, USA, 2011.
5. Ang, S.; Oliva, A. *Power—Switching Converters*; CRC Press Taylor and Francis Group: Boca Raton, FL, USA, 2011.
6. Blaabjerg, F.; Dragicevic, T.; Davari, P. Applications of power electronics. *Electronics* **2019**, *8*, 465. [CrossRef]
7. Górecki, K.; Zarębski, J. The method of a fast electrothermal transient analysis of single-inductance dc-dc converters. *IEEE Trans. Power Electron.* **2012**, *27*, 4005–4012. [CrossRef]

8. Detka, K.; Górecki, K.; Zarębski, J. Modeling single inductor dc—dc converters with thermal phenomena in the inductor taken into account. *IEEE Trans. Power Electron.* **2017**, *32*, 7025–7033. [CrossRef]
9. Starzak, Ł.; Zubert, M.; Janicki, M.; Torzewicz, T.; Napieralska, M.; Jabłoński, G.; Napieralski, A. Behavioral approach to SiC MPS diode electrothermal model generation. *IEEE Trans. Electron Devices* **2013**, *60*, 630–638. [CrossRef]
10. Górecki, P.; Górecki, K. Electrothermal Averaged Model of a Diode-Transistor Switch Including IGBT and a Rapid Switching Diode. *Energies* **2020**, *13*, 3033. [CrossRef]
11. Blaabjerg, F.; Jaeger, U.; Munk-Nielsen, S.; Pedersen, J.K. Power Losses in PWM-VSI Inverter Using NPT or PT IGBT Devices. *IEEE Trans. Power Electron.* **1995**, *10*, 358–367. [CrossRef]
12. Codecasa, L.; d'Alessandro, V.; Magnani, A.; Irace, A. Circuit-Based Electrothermal Simulation of Power Devices by an Ultrafast Nonlinear MOR Approach. *IEEE Trans. Power Electron.* **2016**, *31*, 5906–5916. [CrossRef]
13. di Napoli, F.; Magnani, A.; Coppola, M.; Guerriero, P.; D'Alessandro, V.; Codecasa, L.; Tricoli, P.; Daliento, S. On-Line Junction Temperature Monitoring of Switching Devices with Dynamic Compact Thermal Models Extracted with Model Order Reduction. *Energies* **2017**, *10*, 189. [CrossRef]
14. Basso, C. *Switch-Mode Power Supply SPICE Cookbook*; McGraw-Hill: New York, NY, USA, 2001.
15. Maksimovic, D.; Stankovic, A.M.; Thottuvelil, V.J.; Verghese, G.C. Modeling and simulation of power electronics converters. *Proc. IEEE* **2001**, *89*, 898–912. [CrossRef]
16. Maksimović, D. Automated steady-state analysis of switching power converters using a general-purpose simulation tool. In Proceedings of the PESC97. Record 28th Annual IEEE Power Electronics Specialists Conference. Formerly Power Conditioning Specialists Conference 1970-71. Power Processing and Electronic Specialists Conference 1972, St. Louis, MO, USA, 27 June 1997; Volume 2, pp. 1352–1358.
17. Górecki, P.; Wojciechowski, D. Accurate Computation of IGBT Junction Temperature in PLECS. *IEEE Trans. Electron Devices* **2020**, *67*, 2865–2871. [CrossRef]
18. Perret, R. *Power Electronics Semiconductor Devices*; John Wiley and Sons: Hoboken, NJ, USA, 2009.
19. Rashid, M.H. *Spice for Power Electronics and Electric Power*; CRC Press: Boca Raton, FL, USA, 2006.
20. Azer, P.; Emadi, A. Generalized State Space Average Model for Multi-Phase Interleaved Buck, Boost and Buck-Boost DC-DC Converters: Transient, Steady-State and Switching Dynamics. *IEEE Access.* **2020**, *8*, 77736–77745. [CrossRef]
21. Mawby, P.A.; Igic, P.M.; Towers, M.S. Physically based compact device models for circuit modelling applications. *Microelectron. J.* **2001**, *32*, 433–447. [CrossRef]
22. AHefner, R.; Blackburn, D.L. Simulating the Dynamic Electrothermal Behavior of Power Electronic Circuits and Systems. *IEEE Trans. Power Electron.* **1993**, *8*, 376–385. [CrossRef]
23. D'alessandro, V.; Codecasa, L.; Catalano, A.P.; Scognamillo, C. Circuit-Based Electrothermal Simulation of Multicellular SiC power MOSFETs using FANTASTIC. *Energies* **2020**, *13*, 4563. [CrossRef]
24. Zarębski, J.; Górecki, K. The electrothermal large-signal model of power MOS transistors for SPICE. *IEEE Trans. Power Electron.* **2010**, *25*, 1265–1274. [CrossRef]
25. Ammous, A.; Ammous, K.; Morel, H.; Allard, B.; Bergogne, D.; Sellami, F.; Chante, J.P. Electrothermal modeling of IGBTs: Application to short-circuit conditions. *IEEE Trans. Power Electron.* **2000**, *15*, 778–790. [CrossRef]
26. Vorperian, V. *Fast Analitycal Techniques for Electrical and Electronic Circuits*; Cambridge University Press: Cambridge, UK, 2002.
27. Bedrosian, D.; Vlach, J. Time-domain analysis of networks with internally controlled switches. *IEEE Trans. Circuits Syst. I Fund. Theory Appl.* **1992**, *39*, 199–212. [CrossRef]
28. Han, J.; Zhang, B.; Qiu, D. Bi-switching Status Modeling Method for DC-DC Converters in CCM and DCM Operations. *IEEE Trans. Power Electron.* **2017**, *21*, 2464–2472. [CrossRef]
29. Ben-Yaakov, S.; Gaaton, Z. Generic SPICE compatible model of current feedback in switch mode converters. *Electron. Lett.* **1992**, *28*, 1356–1358. [CrossRef]
30. Górecki, K. A New Electrothermal Average Model of the Diode-Transistor Switch. *Microel. Reliab.* **2008**, *48*, 51–58. [CrossRef]
31. Górecki, P. Application of the Averaged Model of the Diode-transistor Switch for Modelling Characteristics of a Boost Converter with an IGBT. *Int. J. Electron. Telecommun.* **2020**, *66*, 555–560.
32. Górecki, K.; Detka, K. Application of Average Electrothermal Models in the SPICE-Aided Analysis of Boost Converters. *IEEE Trans. Ind. Electron.* **2019**, *66*, 2746–2755. [CrossRef]
33. Ben-Yaakov, S. Behavioral Average Modeling and Equivalent Circuit Simulation of Switched Capacitors Converters. *IEEE Trans. Power Electron.* **2011**, *27*, 632–636. [CrossRef]
34. Ayachit, A.; Kazimierczuk, M.K. Averaged Small-Signal Model of PWM DC-DC Converters in CCM Including Switching Power Loss. *IEEE Trans. Circuits Syst. II Express Briefs* **2019**, *66*, 262–266. [CrossRef]
35. Górecki, K. Non-linear average electrothermal models of buck and boost converters for SPICE. *Microelectron. Reliab.* **2009**, *49*, 431–437. [CrossRef]
36. Górecki, P.; Górecki, K. Analysis of the usefulness range of the averaged electrothermal model of a diode-transistor switch to compute the characteristics of the boost converter. *Energies* **2021**, *14*, 154. [CrossRef]
37. Górecki, K.; Zarębski, J.; Górecki, P.; Ptak, P. Compact Thermal Models of Semiconductor Devices–A Review. *Int. J. Electron. Telecommun.* **2019**, *65*, 151–158.
38. Szekely, V. A new evaluation method of thermal transient measurement results. *Microelectron. J.* **1997**, *28*, 277–292. [CrossRef]

39. Bagnoli, P.E.; Casarosa, C.; Ciampi, M.; Dallago, E. Thermal Resistance Analysis by Induced Transient (TRAIT) Method for Power Electronic Devices Thermal Characterization—Part I: Fundamentals and Theory. *IEEE Trans. Power Elect.* **1998**, *13*, 1208–1219. [CrossRef]
40. Vassighi, A.; Sachder, M. *Thermal and Power Management of Integrated Circuits*; Springer: Berlin, Germany, 2006.
41. Górecki, K.; Górecki, P.; Zarębski, J. Measurements of parameters of the thermal model of the IGBT module. *IEEE Trans. Instrum. Meas.* **2019**, *68*, 4864–4875. [CrossRef]
42. Schweitzer, D.; Ender, F.; Hantos, G.; Szabo, P.G. Thermal transient characterization of semiconductor devices with multiple heat-sources—Fundamentals for a new thermal standard. *Microelectron. J.* **2015**, *46*, 174–182. [CrossRef]
43. Oettinger, F.F.; Blackburn, D.L. *Semiconductor Measurement Technology: Thermal Resistance Measurements*; U.S. Department of Commerce: Washington, DC, USA, 1990; NIST/SP-400/86.